Effect of the Insertion of a Glycine Residue into the Loop Spanning Residues 536−541 on the Semiquinone State and Redox Properties of the Flavin Mononucleotide-Binding Domain of Flavocytochrome P450BM-3 from *Bacillus megaterium*

Huai-Chun Chen[‡] and Richard P. Swenson*[,‡,§]

Department of Biochemistry and Ohio State Biochemistry Program, The Ohio State University, Columbus, Ohio 43210

Received May 20, 2008; Revised Manuscript Received November 7, 2008

ABSTRACT: Despite sharing sequence and structural similarities with other diflavin reductases such as NADPH-cytochrome P450 reductase (CPR) and nitric oxide synthase, flavocytochrome P450BM-3 displays some unique redox and electron transferring properties, including the inability to thermodynamically stabilize the neutral semiquinone (SQ) state of the flavin mononucleotide (FMN) cofactor. Rather, the anionic SQ species is only transiently formed during rapid reduction. Why is this? The absence of a conserved glycine residue and, as a consequence, the shorter and less flexible cofactor-binding loop in P450BM-3 represents a notable difference from other diflavin reductases and the structurally related flavodoxin. This difference may facilitate the formation of a strong hydrogen bond between backbone amide NH group of Asn537 and N5 of the oxidized FMN, an interaction not found in the other proteins. In the flavodoxin, the conserved glycine residue plays a crucial role in a redox-linked conformational change that contributes to the thermodynamic stabilization of the neutral SQ species of the FMN through the formation of a hydrogen bond with the N5H group of the flavin. In this study, a glycine residue was inserted after Tyr536 in the loop within the isolated FMN-binding domain as well as the diflavin reductase domain of P450BM-3, a position equivalent to Gly141 in human CPR. As a result, the insertion variant was observed to accumulate the neutral form of the FMN SQ species much like CPR. The midpoint potential for the SQ/HQ couple decreased by 68 mV, while that for the OX/SQ couple remained unchanged. ^{15}N NMR data provide evidence of the disruption of the hydrogen bond between the backbone amide group of Asn537 and the N5 atom in the oxidized state of the FMN. Molecular models suggest that the neutral FMN SQ could be stabilized through hydrogen bonding with the backbone carbonyl group of the inserted glycine residue in a manner similar to that of CPR and the flavodoxin. The insertion of the glycine at the same location within the diflavin domain resulted in a purified protein that retained nearly stoichiometric levels of bound FAD but tended to lose the FMN cofactor. This preparation retained one-third of the ferricyanide reductase activity but <1% of the cytochrome *c* reductase activity of the wild type. However, the insertion variant reconstituted with FMN regained nearly half of the wild-type cytochrome *c* reductase activity. These results demonstrate the importance of the unique structural characteristics of the shorter loop in P450BM-3 in establishing the unique redox properties of the FMN in this protein but not its general cytochrome reductase activity.

Flavocytochrome P450BM-3 from *Bacillus megaterium* (CYP102A1) (designated P450BM-3[1] throughout) is a widely studied fatty acid monooxygenase enzyme, both as a model system for understanding eukaryotic P450 systems (*1*) and as a successful molecular template for generating novel catalytic properties of biotechnological value (*2*). P450BM-3 is a multidomain protein consisting of a catalytic N-terminal heme-containing oxygenase domain and a C-terminal reductase domain (designated BMR) that closely resembles the mammalian NADPH-cytochrome P450 reductase (CPR) (*3, 4*). CPR and BMR belong to the diflavin reductase family that utilizes both the FAD and FMN cofactors during electron transfer (*5*) and are thought to have evolved from the fusion of $NADP^+$-ferredoxin reductase and bacterial flavodoxin (*6, 7*). CPR (from rat) and BMR are 33% identical in amino acid sequence and approximately 50% similar in the more highly conserved regions within NADPH and flavin-binding sites (*4, 6*). The FMN-binding domain of P450BM-3 (FBD_{BM3}) shares a similar flavodoxin-like fold with that of CPR (*8*−*10*).

* To whom correspondence should be addressed. Telephone: (614) 292-9428. Fax: (614) 292-6773. E-mail: swenson.1@osu.edu.

‡ Ohio State Biochemistry Program.

§ Department of Biochemistry.

[1] Abbreviations: P450BM-3, flavocytochrome P450BM-3 from *B. megaterium* (CYP102A1); BMR and FBD_{BM3}, reductase (diflavin) domain and FMN-binding domain, respectively, of flavocytochrome P450BM-3 from *B. megaterium*; CPR, mammalian NADPH-cytochrome P450 reductase; FAD, flavin adenine dinucleotide; FMN, flavin mononucleotide; $G537_{ins}$ and BMR-Gly_{ins}, glycine insertion variants in FMN-binding domain and the diflavin reductase domain of P450BM-3, respectively; OX, oxidized; SQ, semiquinone; HQ, hydroquinone.

10.1021/bi800954h CCC: $40.75
Published on Web 12/04/2008

Despite the overall sequence and structural similarities, the redox properties of P450BM-3 are rather distinct from those of CPR and other diflavin reductases. These differences are primarily attributed to the unique characteristics of the FMN-binding site. While both enzymes stabilize the neutral form of the FAD semiquinone (SQ) and have similar midpoint potentials for both one-electron couples of the FAD, the redox properties of the bound FMN cofactor are substantially different. In human CPR, the midpoint potentials of the two one-electron couples of the FMN are well separated, with the oxidized/semiquinone (OX/SQ) couple having the highest value of the four flavin couples in this enzyme ($E_{OX/SQ} = -43$ mV, and $E_{SQ/HQ} = -280$ mV). The neutral form of FMN_{SQ} is thermodynamically stabilized (*11*). In contrast, potentials for the one-electron couples for the FMN in P450BM-3 are more similar, with the highest value assigned to the semiquinone/hydroquinone (SQ/HQ) couple ($E_{OX/SQ} = -206$ mV, and $E_{SQ/HQ} = -177$ mV). Unlike in CPR, the FMN_{SQ} is not thermodynamically stabilized but forms transiently as the anionic species (*12*). The neutral SQ state of the FMN in CPR is relatively air stable, while P450BM-3 is usually purified with both flavin cofactors in the oxidized state (*11, 12*). These differences have suggested that the bacterial enzyme may have evolved distinctly different electron transfer and/or regulatory mechanisms compared to other diflavin reductases. CPR is proposed to cycle in a 1−3−2−1 sequence of reduced states of flavin cofactors (the values represent the total number of electrons within the reductase) (*11*). Both the SQ and HQ states of the FMN are capable of electron transfer to the cytochrome acceptor, with early studies favoring FMN_{HQ} as the primary donor. However, more recent pre-steady-state investigations and kinetic reevaluations suggest that only the neutral FMN_{SQ} redox species is kinetically competent to do so under steady-state turnover conditions (see the arguments in ref *5*). In contrast, BMR cycles through a 0−2−1−0 redox sequence with FMN shuttling between the OX and SQ states. In this case, only the anionic FMN_{SQ} is capable of delivering an electron to the heme (*12*). The thermodynamically more favored FMN_{HQ} in P450BM-3 appears to be ineffective as an electron donor for heme iron reduction, and the enzyme usually becomes catalytically inactive when "over-reduced" to this redox state (*12, 13*).

The lack of stabilization of the FMN_{SQ} species of P450BM-3 has been attributed to the unique environment of the FMN compared to CPR and its structural homologue, the flavodoxin (*8, 9, 14*). For example, the FMN-binding site in P450BM-3 lacks the cluster of acidic amino acids that is found in both CPR and flavodoxin (*8, 14*). A generally negative electrostatic environment provided by these charged residues in the FMN-binding site influences the relative stability of the anionic HQ species in flavodoxin (*15*). The FMN-binding loop adjacent the N5/C4O edge of the isoalloxazine ring in P450BM-3 is shorter by one residue, contains a tandem Pro-Pro sequence, and is thought to be less flexible than its counterpart in CPR (Figure 1) (*9*). Furthermore, the highly conserved glycine residue found in the flavodoxin (Gly57 and Gly61 in *Clostridium beijerinckii* and *Desulfovibrio vulgaris*, respectively), CPR (Gly141), and several other diflavin reductase enzymes is absent in P450BM-3. In the flavodoxin, a redox-linked conformational change involving this glycine residue plays a crucial role in the modulation

A

```
P450BM-3 530 LIVTASY-NGHPPDNAKQFVDWL
CPR      134 VFCMATYGEGDPTDNAQDFYDWL
nNOS     803 LVVTSTFGNGDPPENGEKFGCAL
SR       112 IVVTSTQGEGEPPEEAVALHKFL
MSR       54 VVVVSTTGTGDPPDTARKFVKEI
NR1       55 IFVCATTGQGDPPDNMKNFWRFI
```

B

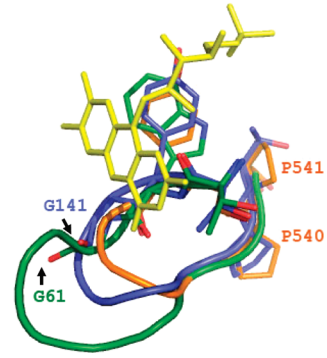

FIGURE 1: (A) Amino acid sequence alignment for the binding region flanking the *re* face of the FMN cofactor for six members of the diflavin reductase family, including flavocytochrome P450BM-3, human cytochrome P450 reductase (CPR), rat neuronal nitric oxide synthase (nNOS), *Escherichia coli* sulfite reductase (SR), human methionine synthase reductase (MSR), and human novel reductase 1 (NR1). Note that the conserved glycine residue highlighted in red is missing in P450BM-3. (B) Structural alignment for the inner FMN-binding loops of *D. vulgaris* flavodoxin [PDB entry 3fx2 (green)], human CPR [PDB entry 1b1c (blue)], and P450BM-3 [PDB entry 1bvy, F chain (orange)]. The flavin cofactor is colored yellow. Note that the loop in P450BM-3 is the shortest one among the three with tandem proline residues situated at the end. The orientations of the carbonyl groups of the conserved glycine residues in CPR and flavodoxin (Gly141 and Gly61, respectively) are indicated by arrows. This figure was generated using PyMOL (*49*).

of the flavin potentials and the thermodynamic stabilization of the neutral flavin SQ through the formation of a hydrogen bond with the N5H group of the FMN (*16*−*18*). A similar role for the equivalent glycine residue has also been proposed in CPR and nitric oxide synthase (*19, 20*). However, unlike CPR and flavodoxin, the shorter loop in FBD_{BM3} places the backbone amide NH group of Asn537 in a position to serve as a hydrogen bond donor to N5 of the FMN in the OX state (*9*). The shorter loop, which adopts a tight β-turn stabilized by two backbone hydrogen bonds, would also seem to preclude a similar redox-linked structural change (*9*).

To test the hypotheses, the FMN-binding loop in FBD_{BM3} was extended by introducing a glycine residue at a position corresponding to residue Gly141 in human CPR and Gly57 in *C. beijerinckii* flavodoxin. This insertion served three purposes. (1) The glycine insertion generates a loop sequence and size that are comparable to those of the other members of the diflavin family. (2) The insertion should disrupt the hydrogen bond with N5 of the FMN in the oxidized state. (3) The expanded loop size and the unique structural features of the glycine residue itself should provide for greater conformational flexibility that could lead to the stabilization of the neutral FMN_{SQ} species through a hydrogen bonding interaction like that in the flavodoxin and CPR. Because of the unique characteristics displayed by this insertion variant, glycine was also introduced into the diflavin reductase domain (BMR) of the monooxygenase to establish its effect on electron transfer activities.

EXPERIMENTAL PROCEDURES

Molecular Cloning and Site-Directed Mutagenesis. The recombinant forms of the FMN-binding domain (amino acids 471−649) as well as the diflavin reductase portion (amino acids 471−1048) of wild-type flavocytochrome P450BM-3 were each cloned separately into the *Eco*RI and *Bam*HI restriction sites of the pT7-7 expression vector (Worthington Biochemical Corp.) and successfully overexpressed in *E. coli* by a variation of previous reports (*12, 21, 22*). The QuikChange site-directed mutagenesis method (Stratagene) was used to generate the glycine insertion variant in the FMN-binding domain (designated throughout as $G537_{ins}$) as well as in the diflavin reductase construct (BMR-Gly_{ins}). The insertion was introduced between Tyr536 and Asn537 within the loop that flanks the N5/C4O edge of the FMN isoalloxazine ring using the oligonucleotide 5′-GTAACGGCGTCT-TATGGCAACGGTCATCCGCC-3′ (forward primer shown; inserted bases are underlined). The insertion and the integrity of the entire open reading frame in all plasmid recombinant constructions were confirmed by automated DNA sequence analysis.

Protein Sample Preparation and Flavin Analysis. The wild-type FBD_{BM3} and $G537_{ins}$ proteins were expressed in the BL21(DE3) strain of *E. coli* and purified as described previously (*21*) except that the proteins were eluted from the DEAE-Sephacel column using a linear gradient from 0 to 500 mM NaCl in 50 mM Tris buffer (pH 7.4) containing 0.1 mM EDTA, 0.05 mM DDT, and 10% glycerol. Fractions containing the protein of interest were pooled, concentrated by ultrafiltration, and subjected to gel permeation chromatography (*21*). Wild-type BMR and BMR-Gly_{ins} were purified by affinity chromatography followed by gel permeation chromatography. The protocol described by Rock et al. (*23*) was used for the affinity chromatography step on 2′,5′-ADP agarose (Sigma) except that different buffer compositions were used: buffer A contained 50 mM Tris (pH 7.7), 0.1 mM EDTA, 0.05 mM dithiothreitol, and 10% glycerol for cell suspension as well as the first wash step; the elution buffer contained buffer A, 20 mM 2′(3′)-AMP, and 100 mM NaCl. The flavin content (FAD and FMN) of the BMR preparations was determined by HPLC using a procedure similar to that described by Marohnic et al. (*24*). Typically, a significant loss of the FMN cofactor was noted for the Gly_{ins} variants during the purification procedure. The weaker FMN binding has been noted by others and may be related, in part, to the significantly higher K_d value for the reduced FMN that was subsequently determined for this variant and our general observation that recombinant flavoproteins are often extracted initially from bacterial cells in the partially reduced state. However, the holoproteins could be reconstituted to various extents by incubation with excess FMN on ice for at least 6 h in the dark. Excess flavin was removed by dialysis against 50 mM sodium phosphate buffer (pH 7.0) for FBD_{BM3} proteins and 100 mM Tris buffer (pH 7.4) for BMR proteins.

Spectral Analyses and Determination of the One-Electron Midpoint Potentials. All ultraviolet−visible absorbance spectra were recorded on a Hewlett-Packard 8453 photodiode array spectrophotometer at 25 °C in 50 mM sodium phosphate buffer (pH 7.0). The anaerobic reduction of the protein samples by sodium dithionite and the determination of midpoint potentials for both the OX/SQ and SQ/HQ couples were performed as described previously (*21*). Anthraquinone 2,6-disulfonate ($E_{m,7} = -184$ mV) and anthraquinone 2-sulfonate ($E_{m,7} = -225$ mV) were used as indicator dyes for establishing the system potential (*25*). Data analysis was performed using SigmaPlot (version 9.01, SYSTAT Software, Inc.). The absorbance at 590 nm (the maximum extinction for the neutral SQ form of the flavin) was plotted as a function of the system potential at each point in the titration and after equilibrium had been established (no further spectral changes). Midpoint potentials for both couples were estimated by fitting the plot to the following equation, which represents a two-electron redox process derived from the Nernst equation and the Beer−Lambert law, as described elsewhere (*11, 22*):

$$A^{590} = \frac{a \times 10^{(E_h - E_1')/59} + b + c \times 10^{(E_2' - E_h)/59}}{1 + 10^{(E_h - E_1')/59} + 10^{(E_2' - E_h)/59}} \quad (1)$$

where A is the total absorbance at 590 nm, a, b, and c are the component absorbance values for oxidized, semiquinone, and reduced flavin, respectively, E_h is the system potential, and E_1' and E_2' are the midpoint potentials for the OX/SQ couple and the SQ/HQ couple, respectively.

Determination of the Dissociation Constant and Binding Free Energy for the FMN Cofactor. The dissociation constant (K_d) for the oxidized FMN was determined at 25 °C by titrating flavin solutions with apoprotein that had been freshly prepared in 50 mM sodium phosphate buffer (pH 7.0) containing 10 mM β-mercaptoethanol (*26*) while monitoring the spectral changes by ultraviolet−visible spectroscopy. The K_d values were determined by nonlinear regression analyses of the absorbance changes at 440 and 494 nm (from the difference spectra) as a function of added apoprotein (*21*). All titration data conformed to a hyperbolic binding isotherm involving a single binding site. The K_d values for the SQ and HQ states, which cannot be determined directly, were calculated using the thermodynamic cycle linking the K_d for the oxidized FMN complex and the midpoint potentials for each couple of the bound and free FMN (*27*).

^{15}N and $^{1}H-^{15}N$ HSQC NMR Spectroscopy. Samples of the $G537_{ins}$ variant reconstituted with ^{15}N-enriched FMN were prepared for both one-dimensional (1D) ^{15}N and two-dimensional (2D) $^{1}H-^{15}N$ HSQC NMR spectroscopy as follows. The ^{15}N-enriched FMN was prepared by the extraction and purification of the cofactor from recombinant *C. beijerinckii* flavodoxin overexpressed in *E. coli* cultured in minimal medium containing $^{15}NH_4Cl$ (*28*). A sample of the lyophilized ^{15}N-enriched FMN was dissolved in a solution containing a 4−5-fold molar excess of the $G537_{ins}$ apoprotein to form the reconstituted holoprotein sample for spectroscopy. Excess apoprotein was added so we could be more certain that all the labeled flavin was bound. For NMR experiments involving the reduced protein, oxygen was removed by extensively flushing the sample with prepurified argon for 30−40 min followed by the addition a slight molar excess of a freshly prepared sodium dithionite solution to ensure complete reduction of the FMN cofactor. Both 1D ^{15}N and 2D $^{1}H-^{15}N$ HSQC NMR experiments were performed on a Bruker DMX 600 MHz NMR spectrometer. 1D ^{15}N NMR spectra were recorded at ambient temperature for the oxidized and reduced protein samples (1 mM each) in 100 mM sodium phosphate buffer (pH 7.0) containing

10% D_2O. The experiments were carried out with a 30° ^{15}N flip angle, inverse-gated ^1H decoupling with a 100 μs ^1H 90° pulse for the WALTZ-16 decoupling sequence, and a recycle time of 3.00 s. The ^{15}N chemical shifts were referenced to an external standard of [^{15}N]urea set at 76.0 ppm. Samples for the 2D $^1H-^{15}N$ HSQC experiment contained approximately 500 μM fully reduced protein in the same buffer as described previously, with 5 mM DTT to reduce the level of protein aggregation or precipitation. The NMR data were acquired using an established protocol (*28*) except that a fast-HSQC pulse sequence (*29*) with ^1H and ^{15}N sweep widths of 9615 and 2432 Hz, respectively, was used for the acquisition of spectra and temperature calibration was performed using methanol. Proton chemical shifts were referenced externally to sodium 2,2-dimethyl-2-silapentane-5-sulfonate (DSS).

Molecular Modeling and Computations. A molecular model of the $G537_{ins}$ protein was built using Swiss-PDB Viewer initially on the basis of the three-dimensional (3D) coordinates of wild-type P450BM-3 (PDB entry 1bvy, chain F) (*9*) and the FMN-binding domain of human CPR (PDB entry 1b1c) (*8*). As a starting point, the polypeptide backbone configuration (ϕ and ψ angles) was set to closely approximate the corresponding loop in CPR, which is similar in size to the corresponding loop in P450BM-3 after the glycine insertion. The geometry of the loop with the insertion was optimized using the AMBER molecular mechanical force field as implemented in the HyperChem modeling package (version 7.5, Autodesk, Inc.) using the Polak-Ribiere conjugate gradient algorithm. A distance-dependent dielectric parameter with a scale factor of 1 was used to simulate solvent effects. Also, 1−4 scale factors of 0.5 with no cutoff for the nonbonded interactions were selected in the calculation. A variety of initial loop structures were geometry optimized until a consistent convergent structure was achieved. The quality of the model was evaluated and compared with those of template structures using PROCHECK (version 3.5) (*31*) and WHAT IF (version 4.99) (*32*).

Cytochrome c and Ferricyanide Reductase Activity of BMR. Cytochrome *c* and ferricyanide reductase steady-state turnover activities for the BMR constructs were determined by established methods (*30*). A typical assay for cytochrome *c* reductase activity was conducted in 100 mM Tris buffer (pH 7.4) containing 100 μM NADPH and 65 μM cytochrome *c*. Reductase activity was calculated using a difference molar extinction coefficient for cytochrome $c_{red}-$cytochrome c_{ox} at 550 nm of 21 mM^{-1} cm^{-1}. Similarly, ferricyanide reductase activity was assayed by replacing cytochrome *c* in the mixture described above with 500 μM potassium ferricyanide. The molar extinction coefficient of 1.02 mM^{-1} cm^{-1} at 420 nm was used to determine the rate of ferricyanide reduction.

RESULTS

Spectral and Redox Properties. The absorbance spectrum of $G537_{ins}$ after reconstitution with FMN exhibited two characteristic flavin absorbance maxima at 374 and 451 nm in the visible region (Figure 2). The absorbance maxima were blue-shifted by 16−17 nm compared to those of wild-type FBD_{BM3} (390 and 468 nm). The shoulder near 480 nm and the broad absorption band between 550 and 700 nm that has been attributed to a weak charge transfer complex between the oxidized flavin ring and the flanking coplanar tryptophan residue were less pronounced than for the wild type (*9*). Such spectral shifts are indicative of greater solvent exposure of the isoalloxazine ring and/or a weakening of hydrogen bonding interactions (*33*).

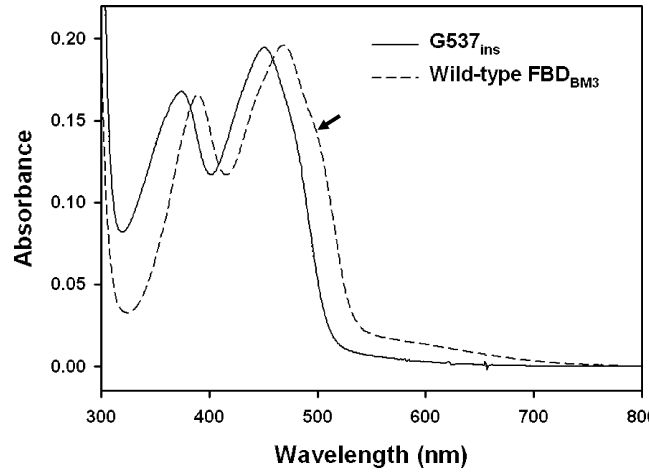

FIGURE 2: Ultraviolet−visible absorption spectra of wild-type FBD_{BM3} (20 μM) (---) and the $G537_{ins}$ variant reconstituted with FMN (18 μM) (—) both in the oxidized state. Both spectra were recorded in 50 mM sodium phosphate buffer (pH 7.0). The shoulder at ~500 nm (indicated by the arrow) and the charger transfer band (550−700 nm) observed in wild-type FBD_{BM3} were less pronounced in $G537_{ins}$.

The spectral changes occurring during the anaerobic reductive titration of $G537_{ins}$ with sodium dithionite were substantially different from those for the wild type (Figure 3). Reduction of wild-type FBD_{BM3} proceeded as a single, two-electron process from the OX to the HQ state, reflected by the appearance of a distinct isosbestic point at 348 nm with no appreciable accumulation of either ionization state of the FMN_{SQ} (Figure 3A) (*34*). The titration of $G537_{ins}$ with sodium dithionite under similar conditions resulted in absorbance decreases at both 451 and 374 nm. However, in marked contrast to that of the wild type, an absorbance band between 520 and 700 nm was observed. This band, with a maximum around 590 nm, has the unmistakable spectral characteristics of the neutral form of the SQ (Figure 3B). The formation of the neutral SQ was fully reversible in that it accumulated to the same extent (approximately 55% of the maximum theoretical formation) when the fully reduced protein was reoxidized with potassium ferricyanide (data not shown). The accumulation of the neutral SQ was a surprising outcome in that wild-type P450BM-3 does not form a stable FMN_{SQ} species, with the anionic form formed only transiently during reduction by dithionite in a stopped-flow spectrophotometer (*12*). There was no evidence of the transient formation or accumulation of the anionic SQ species in the insertion variant. Interestingly, the accumulation of the neutral form of FMN_{SQ} in $G537_{ins}$ was more characteristic of the FMN-binding domain in mammalian CPR (*11*).

The midpoint potentials of both one-electron couples for the $G537_{ins}$ variant were determined by monitoring the spectral changes at 590 nm associated with the formation of the neutral SQ species during anaerobic reductive titrations. Appropriate redox indicator dyes were included to establish the system potential (*21*). The midpoint potentials established for each of the one-electron couples for $G537_{ins}$ were found

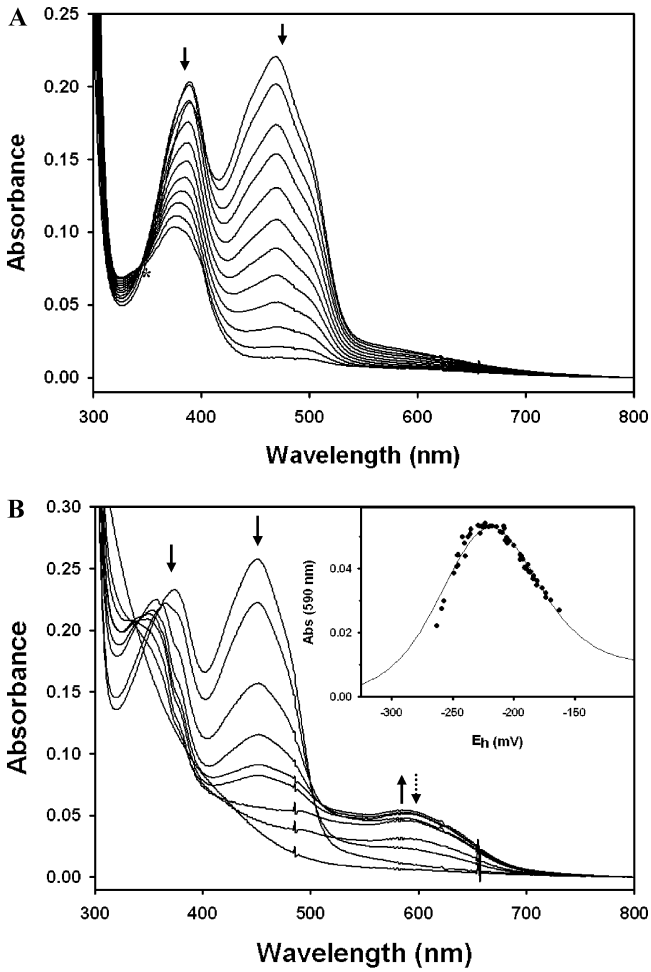

FIGURE 3: Representative ultraviolet−visible absorbance changes during anaerobic reductive titrations of wild-type FBD_{BM3} (A) and $G537_{ins}$ (B) in 50 mM sodium phosphate buffer (pH 7.0). The arrows in both figures show the direction of the spectral change during the titration. A distinct isosbestic point that appeared at 348 nm (indicated by an asterisk) for the wild-type protein was absent for the insertion variant. The inset is a plot of absorbance at 590 nm vs the system potential (E_h) obtained from several titrations for $G537_{ins}$. The midpoint potential for each one-electron couple was estimated by fitting the data to eq 1 as described in Experimental Procedures.

to be reversed compared to those for wild-type FBD_{BM3} (*22*). While the $E_{OX/SQ}$ of $G537_{ins}$ exhibited a value of −198 mV, which is similar to that of wild-type FBD_{BM3} (−206 mV), the $E_{SQ/HQ}$ shifted by >65 mV to a more negative value of −245 mV compared that of the wild type (−177 mV) (Table 1). Interestingly, the midpoint potential for the OX/SQ couple in the $G537_{ins}$ variant remained significantly lower than for the human CPR (−43 mV), while $E_{SQ/HQ}$ became more comparable (−280 mV) (*11*). The potential difference between the one-electron couples of ∼47 mV in the $G537_{ins}$ variant was in close agreement with that calculated from the stability constant (K_s) for the neutral SQ based on its accumulation (∼55%) in both in the reductive and oxidative titrations and the following relationship:

$$K_s = \frac{[FBD_{SQ}]^2}{[FBD_{OX}][FBD_{HQ}]} = \exp\left[\frac{F}{RT}(E^\circ_{OX/SQ} - E^\circ_{SQ/HQ})\right] \quad (2)$$

The extent of accumulation of the neutral SQ and the difference between the midpoint potentials of the two couples are substantially smaller than for those observed in human CPR and *C. beijerinckii* flavodoxin, ∼240 and ∼ 300 mV, respectively (*11, 17*).

Binding of the FMN to $G537_{ins}$ in Each Oxidation State. A feature of wild-type FBD_{BM3} is the rather modest difference in the binding of each of the three oxidation states of the cofactor compared to those of many of the other FMN-binding domains. Binding free energies of −10.1, −10.8, and −10.7 kcal/mol were established for the OX, SQ, and HQ states, respectively (Table 1). The dissociation constant (K_d) for oxidized FMN for the $G537_{ins}$ variant was determined directly by spectrophotometric titrations to be 408 nM. This represents an ∼10-fold increase compared to that for wild-type FBD_{BM3} determined here under similar conditions (41 nM) and the published value of 31 nM from Haines et al. (*26*). This change represents a loss of ∼1.4 kcal/mol of binding free energy. The K_d values for the SQ and HQ states, which cannot be established directly, were calculated from the experimental values for the midpoint potentials for each couple and the K_d for the oxidized FMN based on a linked equilibrium analysis (*27*). The values were determined to be ∼7- and ∼105-fold higher for the SQ and HQ states, respectively, than for wild-type FBD_{BM3} (Table 1). The free energy of binding of the FMN in the SQ state was increased by 0.9 kcal/mol relative to the OX state for the insertion variant. The FMN_{HQ} complex was substantially less stable (by ∼2.7 kcal/mol) than the wild-type protein and ∼1.6 kcal/mol less stable than the SQ complex in $G537_{ins}$. This observation contrasts with that for the wild type, for which there is little difference between the binding of the SQ and HQ species.

^{15}N NMR Studies of $G537_{ins}$. Previous studies of the flavodoxin have shown that while the N5 atom of the FMN is not hydrogen bonded in the oxidized state, a redox-linked conformation change permits the formation of such a bond between a protein backbone carbonyl group and the N5H group of the flavin in both the neutral SQ and HQ states (*17*). This interaction results in the thermodynamic stabilization of neutral FMN_{SQ} and the higher potentials for the OX/SQ couple that characterize these proteins. X-ray crystallographic and NMR spectroscopic studies support a similar peptide backbone-mediated stabilization of these redox states in human CPR (*8, 19*). In contrast, a strong hydrogen bond between the N5 atom of the flavin and the amide NH group of the peptide backbone is already established in the OX state in wild-type FBD_{BM3} (*9*). With those observations in mind, 1D ^{15}N NMR studies were initiated to evaluate the effect of the glycine insertion on the changes in hydrogen bonding and the flavin environment in both OX and HQ states of the FBD_{BM3}. The 1D ^{15}N NMR spectrum of apo$G537_{ins}$ reconstituted with [^{15}N]FMN in the OX state is shown in Figure 4 along with the wild-type FBD_{BM3} spectrum for comparison. Three resonance peaks were observed for the $G537_{ins}$ variant (Figure 4A). The ^{15}N chemical shifts were assigned for the N1, N3, and N10 atoms by comparison to wild-type FBD_{BM3} (*21*) (Figure 4B and Table 2). The resonance for the N5 atom was not as clearly established. A weak signal was occasionally observed in the 310 ppm region; however, the signal-to-noise ratio in this region was poor, and this chemical shift value was outside the typical range for the N5 atom in aqueous and apolar environments (*35*). It is also possible that the N5 resonance has been

Table 1: One-Electron Midpoint Potentials, Dissociation Constants, and Binding Energies for Each Oxidation States of the FMN Cofactor in Wild-Type FBD_{BM3} and $G53_{7ins}$

	midpoint potential (mV)		K_d (μM)[b]			Gibbs free energy (kcal/mol)		
	$E_{OX/SQ}$	$E_{SQ/HQ}$	OX	SQ	HQ	ΔG^{OX}	ΔG^{SQ}	ΔG^{HQ}
wild type	−206[a]	−177[a]	0.041 ± 0.018	0.012	0.014	−10.1	−10.8	−10.7
$G537_{ins}$	−198 ± 11	−245 ± 14	0.41 ± 0.09	0.086	1.47	−8.7	−9.6	−8.0

[a] From ref *22*. [b] K_d values in the OX state were determined by spectrophotometric titration of FMN with apoprotein, and those in the SQ and HQ states were calculated as described in Experimental Procedures (*27*).

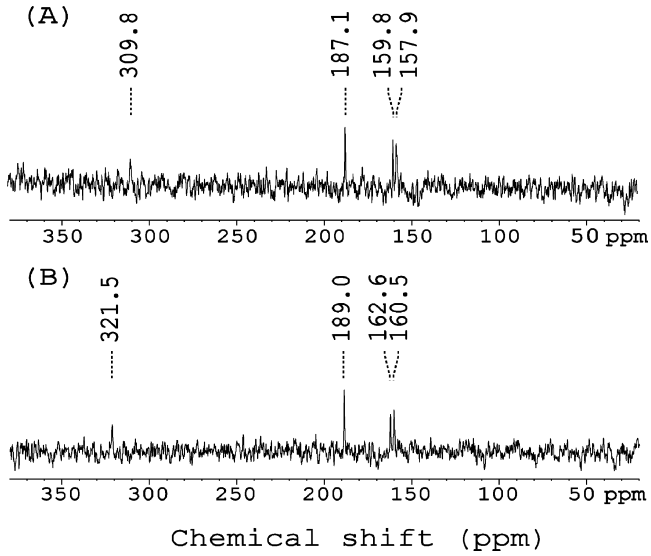

FIGURE 4: (A) 1D ^{15}N NMR spectra of the $G537_{ins}$ variant reconstituted with ^{15}N-enriched FMN in the oxidized state. The ^{15}N chemical shift values of 187.1, 159.8, and 157.9 ppm for the three resonance peaks were assigned to the N1, N10, and N3 atoms of the flavin, respectively. A signal was occasionally observed at ~310 ppm as shown in this spectrum but was not conclusively assigned (see Results). For comparison, the ^{15}N chemical shift values assigned for the N5, N1, N10, and N3 atoms for the FMN bound to wild-type FBD_{BM3} are 321.5, 189.0, 162.6, and 160.5 ppm, respectively (B) (*21*). Both spectra were recorded under similar conditions with the proteins dissolved in 100 mM sodium phosphate buffer (pH 7.0) containing 10% D_2O, and using [^{15}N]urea as the external standard reference.

Table 2: ^{15}N Chemical Shift Values for Free and Bound FMN in the Oxidized State

	^{15}N NMR chemical shift (ppm)			
atom	FMN[a]	TARF[a]	wild-type FBD_{BM3}[b]	$G537_{ins}$
N1	190.8	199.9	189.0	187.1
N3	160.5	159.8	160.5	157.9
N5	334.7	344.3	321.5	(309.8)
N10	164.6	150.2	162.6	159.8

[a] From ref *35*. TARF, tetraacetylriboflavin in $CHCl_3$. [b] From ref *21*.

broadened beyond detection due to conformational flexibility introduced into this region by the insertion, with the resonance at ~310 ppm representing an artifact. Unfortunately, the extension of data recording times beyond 36 h to improve the signal-to-noise ratio in this region resulted in protein precipitation. Nonetheless, the data suggest that the hydrogen bond and the environment of the N5 atom of the FMN have been significantly perturbed in the $G537_{ins}$ variant.

As for wild-type FBD_{BM3}, the ^{15}N chemical shift of the N1 atom in $G537_{ins}$ was shifted upfield relative to FMN in aqueous solution (Table 2). For pyridine-type nitrogen atoms, such shifts are reflective of hydrogen bonding at N1 of the oxidized flavin (*36*). Although pyrrole-type nitrogen atoms such as N3 and N10 of flavin in the OX state are rather insensitive to changes in hydrogen bonding interactions, small downfield shifts do occur in response to such interactions (*36*). The ^{15}N chemical shift for the N3 atom in the insertion variant shifted upfield by ~2.6 ppm (to 157.9 ppm) relative to that of the wild type (Figure 4 and Table 2), reflecting a weaker hydrogen bonding interaction at the N3H group in $G537_{ins}$. The N10 atom of $G537_{ins}$ resonates at 159.8 ppm, which was upfield by ~2.8 ppm from those of FMN in an aqueous environment and wild-type FBD_{BM3}, but downfield from TARF in $CHCl_3$ (Table 2). Because the N10 atom cannot form hydrogen bonds, this upfield shift must be explained in some other manner. The shift could result from a decrease in the degree of sp^2 hybridization if the atom was moved slightly out of the plane of the isoalloxazine ring (*35*) or from a change in the polarization of the isoalloxazine ring due to a weakening of the hydrogen bonding interactions at C2O and C4O (*37*). However, these groups interact with the backbone amide NH group of Gln579 and side chain hydroxyl group of Thr577 in the wild-type domain which are located on an adjacent loop (*9*). The upfield shift of the N10 resonance could also result from the disruption of the hydrogen bond at the N5 atom of the FMN (*35, 37*) as a result of the glycine insertion.

Both the $^{15}N-^{1}H$ coupling constant and ^{15}N chemical shift changes for the fully reduced state of wild-type FBD_{BM3} suggest a high degree of sp^3 character of the N5H group due to the out-of-plane puckering of the central flavin ring, perhaps preventing the potential clash with the backbone amide group of Asn537 in the reduced enzyme (*21*). A similar investigation for the $G537_{ins}$ variant in the reduced state would be intriguing because of our hypothesis that this interaction was disrupted by the insertion. Unfortunately, we were unable to obtain satisfactory results for the reduced $G537_{ins}$ by 1D ^{15}N NMR analyses due to very weak signals typically associated with ^{15}N NMR analyses, the tendency for the sample to reoxidize and precipitate during extended data acquisition times. Alternatively, $^{1}H-^{15}N$ HSQC NMR studies on reduced $G537_{ins}$ were initiated because of its increased sensitivity, although this approach would be responsive to only the N3H and N5H moieties. Only the cross-peak for the N3H group of the reduced $G537_{ins}$ was observed (data not shown). The absence of a signal attributable to the N5H group was consistent with the 1D NMR results, again suggesting a rapid proton exchange with the solvent and/or signal broadening due to rapid changes in its environment. The temperature coefficient ($\Delta\delta/\Delta T$) for the proton chemical shift has been used as an indicator of relative hydrogen bonding strength in that the chemical shift of the amide proton that is exposed to solvent is more sensitive to temperature than those involved in intermolecular hydrogen bonding (*28, 38*). This approach was applied here. The

temperature coefficient for N3H in reduced $G537_{ins}$ was found to be −4.4 ppb/K, a value similar to that for an amide proton involved in an intramolecular hydrogen bond (*39*), but that was 3-fold higher than that determined for the wild type under similar conditions (−1.65 ppb/K). These results indicate that the hydrogen bonding interaction at the N3H group was retained but significantly weakened by the glycine insertion, a conclusion consistent with the 1D NMR data. Unfortunately, the absence of an HSQC signal precluded a similar analysis for the N5H group.

Molecular Modeling. To gain structural insights into how the inner FMN-binding loop of $G537_{ins}$ interacts with its flavin cofactor, a structural model of $G537_{ins}$ was generated. The X-ray crystal structure of wild-type FBD_{BM3} served as the initial template, and because of the general sequence homology of the two loops after the insertion, the FMN-binding domain of CPR was used as a guide (*8, 9*). As a starting point for the model, the backbone torsion angles of seven residues (^{534}A-S-Y-G-N-G-H^{539}) flanking the *re* face of the FMN isoalloxazine ring were initially adjusted to values similar to those of the corresponding residues in CPR with Swiss-PDB Viewer. The modeled loop was then subjected to multiple rounds of geometry optimization using the AMBER molecular mechanical force field and evaluated by structure validation software as described in Experimental Procedures. As a check, the initial structure of the loop was repeatedly adjusted and reoptimized to establish that the loop converged to the final structure reported here.

Compared to the wild-type FBD_{BM3} structure, the final positions of the α-carbon atoms of the loop in the modeled structure of $G537_{ins}$ were more similar to those of the human CPR with a root-mean-square deviation (rmsd) of 0.83 Å (Figure 5A). The inserted glycine residue was situated at a position corresponding to Asn537 in the wild-type structure. Perhaps the most significant structural consequence of the insertion was the dislocation of the backbone amide nitrogen atom of Asn537 to a position that was at least 2.5 Å farther from the N5 atom of the flavin (Figure 5A). This displacement would certainly disrupt the hydrogen bond between Asn537 and the oxidized FMN that is observed in the wild-type structure (*9*). Furthermore, the amide NH group of the inserted glycine was positioned 3.7 Å from the N5 atom, a distance quite comparable to that of Gly141 in human CPR (3.8 Å) and too large for the formation of a new hydrogen bond at this position in the oxidized state, just as observed for human CPR and the flavodoxin (*8*). However, the carbonyl group of the inserted glycine was within a suitable distance to serve as a hydrogen bond acceptor for the N5H group in the reduced states of the FMN. The functional significance of this observation will be discussed below. The rest of the enlarged loop in $G537_{ins}$ appears to be stabilized by maintaining the two hydrogen bonds that are present between the backbone atoms of Tyr536 and His539 that help form a type I′ turn with Gly538 at the third position in the wild type (*9*). However, a different turn conformation was adopted that more closely resembles that of human CPR (Figure 5B). Two tandem proline residues, located at the end of the loop, remain in backbone conformations similar to that in the wild type. The side chain of Tyr536, which stacks on the *re* face of the flavin ring and hydrogen bonds with the phosphate group in wild-type FBD_{BM3} (*9*), was also in a similar position as in the wild-type structure, implying that these interactions can still be maintained in $G537_{ins}$.

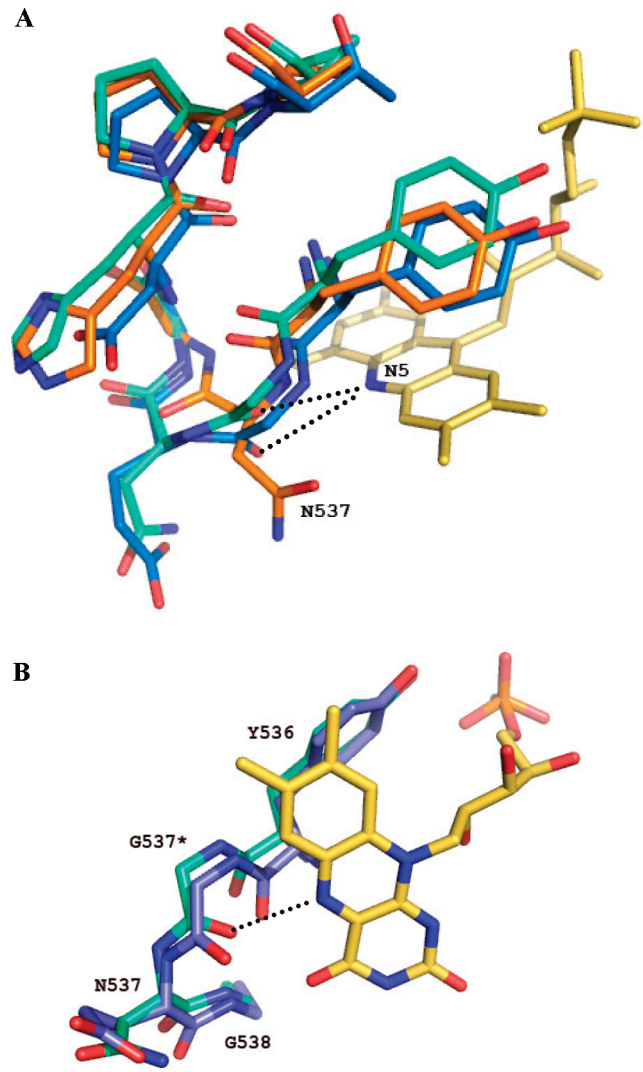

FIGURE 5: (A) Peptide loop of the $G537_{ins}$ model (cyan) flanking the *re* face of the FMN cofactor (yellow) superimposed with the analogous regions of wild-type FBD_{BM3} [PDB entry 1bvy, F chain (orange)] and CPR [PDB entry 1b1c (blue)]. The structure of the loop region of $G537_{ins}$ closely resembles that of the human CPR. Note that Asn537 in the wild-type structure was pushed away from the N5 atom (highlighted in blue) in the modeled structure. Potential hydrogen bonds between N5 and the glycine residues in CPR (G141) and the modeled structure (G537*) are indicated by dashed lines. (B) Superposition of the residues ^{536}Y-G-N-G^{538} in the modeled structure (cyan) and the corresponding residues in CPR (blue). The carbonyl group of the inserted glycine residue (G537*) in the modeled structure was oriented toward the FMN, and the potential hydrogen bond with the N5 atom of the cofactor is indicated by the dashed line. Both figures were generated using PyMOL (*49*).

Electron Transferring Activity of the Diflavin Reductase Domain (BMR) Containing the G537 Insertion. The glycine insertion was initially introduced into just the FMN-binding domain to greatly facilitate the characterization of the effects of this alteration on the redox properties of the bound FMN, the principal goal of this study. However, this construction precluded the investigation of its effects on the electron transferring activities of this protein. The electron transferring characteristics of the diflavin reductase domain (BMR) of flavocytochrome P450BM-3 have been studied extensively

Table 3: Steady-State Kinetic Measurements of the Wild-Type BMR and BMR-Gly$_{ins}$ toward Electron Acceptors

	turnover number (min^{-1})[a]			
		BMR-Gly$_{ins}$		
electron acceptor	wild type	without FMN	with FMN	CPR[b]
ferricyanide	7300 ± 370	2500 ± 120	2000 ± 100[c]	4300
cytochrome *c*	4200 ± 330	11 ± 1	1900 ± 130[d]	2300

[a] Values were determined from at least three independent measurements under the assay conditions described in Experimental Procedures. [b] From ref *50*. [c] Reactions were performed in the presence of a 2-fold molar excess of FMN over BMR-Gly$_{ins}$. [d] From the average maximal rate obtained under the conditions described in the legend of Figure 6.

and have been compared to those of the mammalian CPR. Thus, the glycine insertion was introduced at the level of BMR (i.e., BMR-Gly$_{ins}$) to assess its effects on the cytochrome reductase activity. Unlike for the wild-type BMR prepared in the same way, flavin analyses of the purified BMR-Gly$_{ins}$ protein indicated that while nearly stoichiometric amounts of FAD were bound, nearly all the FMN cofactor was absent as purified. The loss of FMN in BMR-Gly$_{ins}$ was anticipated on the basis of our observations of the loss of FMN during purification and the higher K_d determined for this variant at the FBD$_{BM3}$ level (see above). Partial reconstitution of BMR-Gly$_{ins}$ could be achieved by incubation of the purified protein with a 5-fold excess of FMN followed by dialysis. Flavin analysis revealed that BMR-Gly$_{ins}$ could be partially reconstituted but retained only 0.17 mol of FMN per mole of enzyme (and FAD) under these conditions. These results are corroborated by the activity measurements below and are also consistent with the inability to fully reconstitute the FBD$_{BM3}$ with FMN. The reasons for the incomplete reconstitution of the glycine insertion variants are not known at this time.

Steady-state turnover measurements were initially performed for BMR-Gly$_{ins}$ toward an external electron acceptor, cytochrome *c*, in the absence and the presence of free FMN. As purified, BMR-Gly$_{ins}$ displayed <1% of the cytochrome *c* reductase activity of the wild-type BMR (11 ± 1 and 4200 ± 330 min^{-1} for BMR-Gly$_{ins}$ and wild-type BMR, respectively) (Table 3). This result was not surprising given the near absence of FMN in this preparation. The specific activity did increase by at least 23-fold upon incubation with an excess of FMN (to a value of 260 ± 81 min^{-1} based on the total amount of the BMR-Gly$_{ins}$ protein added to the assay), but still only recovering ~6% of that for the wild-type reductase. The reduced activity seemed to correlate with the level of reconstitution of BMR-Gly$_{ins}$ with FMN as described above. To be more certain of the true activity of the reconstituted variant under controlled conditions to monitor complete reconstitution, the cytochrome *c* reductase activity was assayed as follows. Stock solutions containing increasing levels of the BMR-Gly$_{ins}$ protein (as purified lacking the bound FMN) and a constant concentration of free FMN were preincubated for at least 1 h on ice prior to assaying for cytochrome *c* reductase activity. The activity was observed to increase in proportion to the amount of protein present until a maximal activity was achieved, presumably when all the FMN was bound (Figure 6). However, this level was first attained when the total protein concentration was ~9-fold greater than that of the added FMN. Under these

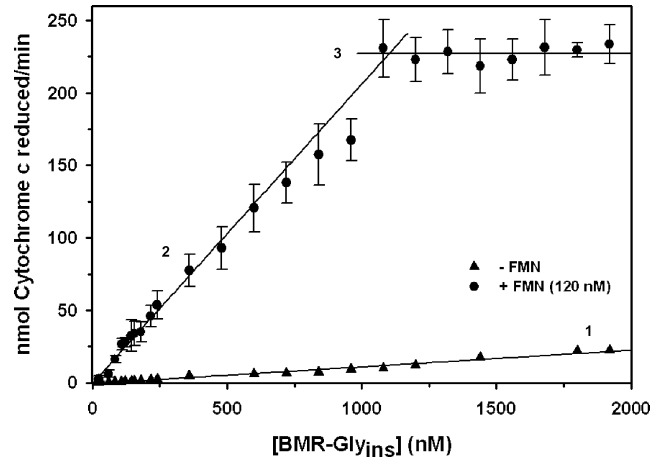

FIGURE 6: Reconstitution of cytochrome *c* reductase activity for BMR-Gly$_{ins}$. Increasing levels (from 24 nM to 1.92 μM) of the BMR-Gly$_{ins}$ protein (as purified lacking the bound FMN) were preincubated for 1 h on ice either in the absence (▲) or in the presence of a constant concentration of free FMN (120 nM) (●) prior to assaying for cytochrome *c* reductase activity in 100 mM Tris buffer (pH 7.4) at 25 °C as described in Experimental Procedures. Each data point represents the average (±standard deviation) of at least three independent determinations in the presence of FMN. The specific reductase activities based on total protein assayed were derived from the slope for each set of enzyme assays [lines 1 and 2; 11 ± 1 and 200 ± 5 mol min^{-1} (mol of protein)$^{-1}$, respectively]. The specific activity of the fully reconstituted BMR-Gly$_{ins}$ was estimated to be 1900 ± 130 mol min^{-1} (mol of holoenzyme)$^{-1}$ based on the maximum activity that was attained when the FMN apparently became limiting (line 3) and a maximal level of holoenzyme was formed. Maximal activity was reached when a 9-fold excess of BMR-Gly$_{ins}$ protein was added (intercept of lines 2 and 3), suggesting that only ~11% of the protein could be reconstituted with FMN under these conditions.

conditions, it was expected that if all the protein was capable of binding the FMN, maximal activity would be achieved when the concentration of the added protein was equal to that of the FMN in solution. These data provide persuasive evidence that only ~11% of BMR-Gly$_{ins}$ is capable of binding FMN and, thus, regaining reductase activity. In light of this, the specific activity of the reconstituted holoprotein was calculated to be 1900 ± 130 min^{-1} or ~45% of that of wild-type BMR assayed under similar conditions.

In addition to cytochrome *c* reductase activity, ferricyanide reductase activity was also determined for BMR-Gly$_{ins}$. While the presence of both FMN and FAD is required for the reduction of cytochrome *c*, it has been shown that the reduction of ferricyanide depends only on the FAD domain in wild-type P450BM-3 (*30*). The FMN-deficient BMR-Gly$_{ins}$ exhibits 34% of the wild-type ferricyanide reductase activity in the absence of free FMN (2500 ± 120 and 7300 ± 370 min^{-1} for BMR-Gly$_{ins}$ and the wild type, respectively). Interestingly, the insertion variant exhibits slightly decreased ferricyanide reductase activity (2000 ± 100 min^{-1}) in the presence of a 2-fold excess of FMN (Table 3).

DISCUSSION

The unique properties of flavocytochrome P450BM-3 provide an excellent means of improving our knowledge of the mechanisms by which flavoproteins modulate the redox and physicochemical properties of the bound flavin cofactor, a long-term focus of this laboratory. The absence of a conserved glycine residue in the shortened loop of

P450BM-3 when compared to the flavodoxin-like FMN-binding domains of several diflavin reductase enzymes such as the mammalian CPR (*8, 10*), nitric oxide synthase (*20*), novel reductase 1 (*40*), methionine synthase reductase (*41*), and bacterial sulfite reductase (*42*) (Figure 1A) served as the target for this study. The results obtained provide both general insights into the various mechanisms by which flavoproteins regulate the redox properties of the flavin cofactor(s) and the electron transfer activities of diflavin reductases.

In the flavodoxin, the equivalent glycine is known to be crucial in establishing the redox potentials and properties of the bound flavin cofactor (*14, 18, 43*−*45*). A redox-linked reorientation of the backbone carbonyl group of this residue from a position in which the carbonyl oxygen is pointed away from the flavin ring (designated the "O-down" configuration) to the "O-up" configuration in the reduced states establishes a new hydrogen bond with the N5H group of the reduced FMN (*17*). This structural rearrangement closely resembles a type II to type II′ turn transition for which a glycine residue is favored at the second position in the turn. Substitutions with amino acid residues with side chains even as small as the methyl group of alanine for the conserved glycine residues in the flavodoxins from *C. beijerinckii* and *D. vulgaris* (Gly57 and Gly61, respectively) perturb the redox potentials of the FMN and reduce the stability of the SQ state (*16, 17, 28*). A compelling correlation has been observed between the $E_{OX/SQ}$ and the conformational energetics of the reverse turn, further demonstrating the functional importance of this glycine residue (*17, 46*). NMR studies of the FMN-binding domain in human CPR in the three oxidation states suggest that a similar redox-linked conformational change involving Gly141 mediates the stabilization of the neutral SQ species in this reductase as well (*19*).

Molecular models suggested that the insertion of a glycine residue after the tyrosine within the ^{536}Y-N-G-H^{539} loop in P450BM-3 should generate a loop structure more like that found in CPR (*8, 9*) (Figure 5). The insertion was predicted to disrupt the type I′ turn configuration and extend the protein backbone away from the flavin ring, leading to the weakening or elimination of the hydrogen bonding interaction with the FMN. This conclusion was supported by the loss the NMR signal for the N5 atom, the upfield chemical shift for the N10 atom, the UV−visible spectral changes, and an observed loss of ∼1.4 kcal/mol in binding free energy for the oxidized state (Table 1). However, the most noticeable consequence of the insertion was the accumulation of the neutral form of the FMN_{SQ} during the anaerobic reductive titration of $G537_{ins}$. This observation is in marked contrast to that with the wild-type protein which only transiently forms the anionic semiquinone. Thus, the glycine insertion has generated a FMN-binding domain in P450BM-3 that exhibits redox characteristics more like those of the mammalian CPR. When CPR is reduced by two electron equivalents, the FAD and FMN cofactors rapidly equilibrate with each flavin achieving the neutral SQ state, generating the so-called disemiquinoid species that is characteristic of this reductase (*11*). The appearance of the neutral FMN_{SQ} in $G537_{ins}$ signaled a significant change in the ionization state of the SQ species compared to the wild type. The pK_a of the flavin SQ in solution is reported to be 8.6 (*47*). In wild-type FBD_{BM3}, the pK_a of the bound FMN must be at least two pH units lower because only the anionic species is observed. For $G537_{ins}$, the characteristic absorbance spectrum for the neutral SQ persisted during rapid mixing of the partially reduced protein with buffers with increasing pH values in a stopped-flow spectrophotometer, indicating that the glycine insertion has caused the pK_a of the FMN_{SQ} to increase to a value of >12 (data not shown). In the *C. beijerinckii* flavodoxin, the pK_a of the neutral SQ has been estimated to be >13 (*17*). This substantial increase was attributed primarily to the strong hydrogen bonding interaction between the N5H group of the neutral FMN_{SQ} after it was noted that the pK_a was lowered by at least two pH units in the G57T variant which disrupts this interaction (*17*). The increase in the pK_a of the FMN_{SQ} in the $G537_{ins}$ variant can be rationalized in part by a disruption of the hydrogen bonding interaction between the amide NH group of Asn537 and the N5 atom of the FMN if preserved in the SQ state of the wild-type protein. The expansion of the loop would also result in a greater solvent exposure of the flavin ring.

However, the rather dramatic increase in the pK_a implied by the pH jump analyses implies that a new hydrogen bond is formed between the carbonyl group of the inserted glycine and the N5H group of the neutral SQ species as observed in the flavodoxin. Our molecular model does show that the carbonyl group of the inserted glycine residue is oriented toward the flavin and within hydrogen bonding distance of the N5H group (Figure 5). This interaction has been estimated to contribute up to 4.0 kcal/mol to the stabilization of the relatively air stable neutral SQ species in the flavodoxin (*28*). However, the degree of stabilization in the $G537_{ins}$ variant appears to be lower as reflected by a narrower separation of the midpoint potentials between two one-electron couples and the lower levels of accumulation of the radical at equilibrium during reductive titrations. Just as for wild-type FBD_{BM3}, the binding free energy for the neutral SQ state was only modestly higher than for the OX state (by 0.9 kcal/mol) (Table 1) compared to a differential stabilization of the neutral radical in the flavodoxin of 3.3 kcal/mol (*28*). These observations suggest that should a hydrogen bonding interaction be formed with the N5H group of the FMN_{SQ} in $G537_{ins}$, it is weaker than in the flavodoxin. This conclusion is supported by the ^{15}N NMR evidence of a weaker hydrogen bond to the N3H group compared to the wild-type protein studies of the variant in both the oxidized and reduced states. In the flavodoxin, changes in interactions with the FMN N3H group can reflect those at the N5 atom (*38*).

A somewhat surprising outcome was that the glycine insertion had the greatest effect on the stability of the FMN_{HQ}. The midpoint potential for the SQ/HQ couple became substantially more negative than for the wild type and the OX/SQ couple in the variant, reflecting a loss of binding energy of ∼2.7 kcal/mol for the FMN_{HQ} species relative to the wild type (Table 1). This observation is not easily explained, yet certain factors may contribute. At least a portion of this difference can be attributed to the reduction of the neutral SQ for $G537_{ins}$ rather than

the anionic species in the wild-type protein. Reduction would be accompanied by differences in the charge distribution in the flavin isoalloxazine ring in each case. Computational studies suggest that the $E_{SQ/HQ}$ in the flavodoxin is not only dependent on the general electrostatic environment of the cofactor but also quite sensitive to the backbone configuration of the analogous loop in those proteins including the orientation of the backbone carbonyl group of the conserved glycine (*48*). The marked sensitivity of HQ state to even relatively subtle changes in the structure of the cofactor binding site has been noted previously in the flavodoxin (*17*). Therefore, altering the local backbone environment by expanding the size and structure of the loop in the FBD_{BM3} could certainly account for the lower stability of the HQ complex.

The differences in redox properties of primarily the FMN cofactor in BM3 could form the basis for differing electron transferring mechanisms and/or regulatory phenomena (*5, 22*). As an initial effort to address some of these issues, steady-state electron transfer activities were evaluated for the glycine insertion introduced into the diflavin reductase domain (BMR) to assess its effect on electron transfer toward electron acceptors ferricyanide and cytochrome *c* and for comparison to mammalian CPR and other diflavin reductases. Our kinetic analyses were complicated by the observation that only a portion (up to 20%) of the recombinant BMR-Gly_{ins} protein was able to fully incorporate FMN to form the holoenzyme. Although the reason for this is not known, it is quite possible that not all of the protein is able to fold properly, particularly in the FMN domain region. FAD binding seems not to be impaired, however, as nearly stoichiometric levels of this cofactor were observed in the purified preparations. The functionality of the FAD domain was confirmed by the observed ferricyanide reductase activity in the insertion variant, albeit at a somewhat reduced level relative compared to the wild-type BMR. Although it is not understood, previous studies have suggested that the ability to transfer electrons from NADPH to FAD to ferricyanide might be affected by FMN deficiency in the FMN-depleted P450BM-3 mutants, which is the case here (*30*).

The evaluation of the cytochrome *c* reductase activity was made more challenging by of the incomplete reconstitution of the BMR-Gly_{ins} protein with the FMN cofactor, which is the primary donor to the cytochrome. However, the turnover number for the holoprotein that could be fully constituted was established from the maximal activity achieved under limiting levels of added FMN (Figure 6). The turnover number obtained in this manner, 1900 $\pm$ 130 min^{-1}, indicates that the insertion variant retained approximately half of the wild-type cytochrome *c* reductase activity, which was more comparable to that of CPR obtained under similar assay conditions (2300 min^{-1}) (*50*). It is generally accepted that only the anionic FMN_{SQ} is capable of delivering an electron to the cytochrome acceptor in BM3 and BMR (*12*). The more thermodynamically favored FMN_{HQ} is believed not to be kinetically competent to do so, forming at a rate slower than the rate of reduction of cytochrome acceptors (*13*). The FMN_{SQ} formed in mammalian CPRs, in this case as the thermodynamically stable neutral form, serves as the electron donor to the cytochrome (*5*). Conversion of BMR into a reductase displaying more CPR-like properties for the FMN cofactor was not, therefore, expected to preclude electron transfer since both types of reductases are capable of doing so. Thus, the alterations of the protonation state and the relative stability of the FMN_{SQ} or the midpoint potentials of the FMN in BMR-Gly_{ins} did not appreciably affect the overall electron transfer activity toward this acceptor. However, other steps in the catalytic pathway are thought to be rate-limiting, including NADPH binding and hydride ion transfer from NADPH to FAD, etc. (*5*), which likely mask changes in the inter-flavin and/or cytochrome electron transfer steps. Although not fully understood for either reductase, the mechanisms and kinetics of electron transfer to their physiological redox partners will likely be different from those determined for cytochrome *c* reduction. It seems plausible that the differing properties of the FMN cofactor and its binding site in BM3 have evolved for specific purposes in this enzyme and the insertion variant will need to be generated and studied at the monooxygenase level. Such studies are being initiated.

In conclusion, the results of this study support the hypothesis that the shorter loop that flanks the *re* face of the FMN in flavocytochrome P450BM-3 promotes the formation of a strong hydrogen bond to the N5 atom of the FMN in the oxidized state and that this interaction was maintained upon reduction to the anionic SQ. The expansion of this loop by the insertion of a glycine residue at a position where such a residue is highly conserved disrupted this interaction and promoted the formation and accumulation of the neutral form of SQ as observed in CPR, the flavodoxins, and other flavoproteins. These results also support our hypothesis on the importance of the structural role of the FMN-binding loop underlying the unique redox properties of P450BM-3 compared to those of CPR. Our functional studies suggest that the insertion within the reductase (BMR) does not significantly affect its general electron transfer activity. However, additional experiments in the full-length P450BM-3 protein are needed to improve our understanding of its effect on the electron transfer during fatty acid hydroxylation. Finally, the results of this study further expand our understanding of the specific structural features that are responsible for establishing the redox properties of flavoproteins.

ACKNOWLEDGMENT

We thank Dr. Chunhua Yuan of the Campus Chemical Instrument Center for assisting in NMR data collection.

REFERENCES

1. Munro, A. W., Leys, D. G., McLean, K. J., Marshall, K. R., Ost, T. W., and Daff, S. (2002) P450 BM3: The very model of a modern flavocytochrome. *Trends Biochem. Sci. 27*, 250–257.
2. Yun, C. H., Kim, K. H., Kim, D. H., Jung, H. C., and Pan, J. G. (2007) The bacterial P450 BM3: A prototype for a biocatalyst with human P450 activities. *Trends Biotechnol. 25*, 289–298.
3. Narhi, L. O., and Fulco, A. J. (1986) Characterization of a catalytically self-sufficient 119,000-dalton cytochrome P-450 monooxygenase induced by barbiturates in *Bacillus megaterium*. *J. Biol. Chem. 261*, 7160–7169.
4. Ruettinger, R. T., Wen, L. P., and Fulco, A. J. (1989) Coding nucleotide, 5′ regulatory, and deduced amino acid sequences of

P-450BM-3, a single peptide cytochrome P-450:NADPH-P-450 reductase from *Bacillus megaterium*. *J. Biol. Chem. 264*, 10987–10995.
5. Murataliev, M. B., Feyereisen, R., and Walker, F. A. (2004) Electron transfer by diflavin reductases. *Biochim. Biophys. Acta 1698*, 1–26.
6. Porter, T. D. (1991) An unusual yet strongly conserved flavoprotein reductase in bacteria and mammals. *Trends Biochem. Sci. 16*, 154–158.
7. Porter, T. D., and Kasper, C. B. (1986) NADPH-cytochrome P-450 oxidoreductase: Flavin mononucleotide and flavin adenine dinucleotide domains evolved from different flavoproteins. *Biochemistry 25*, 1682–1687.
8. Zhao, Q., Modi, S., Smith, G., Paine, M., McDonagh, P. D., Wolf, C. R., Tew, D., Lian, L. Y., Roberts, G. C., and Driessen, H. P. (1999) Crystal structure of the FMN-binding domain of human cytochrome P450 reductase at 1.93 Å resolution. *Protein Sci. 8*, 298–306.
9. Sevrioukova, I. F., Li, H., Zhang, H., Peterson, J. A., and Poulos, T. L. (1999) Structure of a cytochrome P450-redox partner electron-transfer complex. *Proc. Natl. Acad. Sci. U.S.A. 96*, 1863–1868.
10. Wang, M., Roberts, D. L., Paschke, R., Shea, T. M., Masters, B. S., and Kim, J. J. (1997) Three-dimensional structure of NADPH-cytochrome P450 reductase: Prototype for FMN- and FAD-containing enzymes. *Proc. Natl. Acad. Sci. U.S.A. 94*, 8411–8416.
11. Munro, A. W., Noble, M. A., Robledo, L., Daff, S. N., and Chapman, S. K. (2001) Determination of the redox properties of human NADPH-cytochrome P450 reductase. *Biochemistry 40*, 1956–1963.
12. Sevrioukova, I., Shaffer, C., Ballou, D. P., and Peterson, J. A. (1996) Equilibrium and transient state spectrophotometric studies of the mechanism of reduction of the flavoprotein domain of P450BM-3. *Biochemistry 35*, 7058–7068.
13. Murataliev, M. B., Klein, M., Fulco, A., and Feyereisen, R. (1997) Functional interactions in cytochrome P450BM3: Flavin semiquinone intermediates, role of NADP(H), and mechanism of electron transfer by the flavoprotein domain. *Biochemistry 36*, 8401–8412.
14. Watt, W., Tulinsky, A., Swenson, R. P., and Watenpaugh, K. D. (1991) Comparison of the crystal structures of a flavodoxin in its three oxidation states at cryogenic temperatures. *J. Mol. Biol. 218*, 195–208.
15. Zhou, Z., and Swenson, R. P. (1996) The cumulative electrostatic effect of aromatic stacking interactions and the negative electrostatic environment of the flavin mononucleotide binding site is a major determinant of the reduction potential for the flavodoxin from *Desulfovibrio vulgaris* [Hildenborough]. *Biochemistry 35*, 15980–15988.
16. O'Farrell, P. A., Walsh, M. A., McCarthy, A. A., Higgins, T. M., Voordouw, G., and Mayhew, S. G. (1998) Modulation of the redox potentials of FMN in *Desulfovibrio vulgaris* flavodoxin: Thermodynamic properties and crystal structures of glycine-61 mutants. *Biochemistry 37*, 8405–8416.
17. Ludwig, M. L., Pattridge, K. A., Metzger, A. L., Dixon, M. M., Eren, M., Feng, Y., and Swenson, R. P. (1997) Control of oxidation-reduction potentials in flavodoxin from *Clostridium beijerinckii*: The role of conformation changes. *Biochemistry 36*, 1259–1280.
18. Smith, W. W., Burnett, R. M., Darling, G. D., and Ludwig, M. L. (1977) Structure of the semiquinone form of flavodoxin from *Clostridum* MP. Extension of 1.8 Å resolution and some comparisons with the oxidized state. *J. Mol. Biol. 117*, 195–225.
19. Barsukov, I., Modi, S., Lian, L. Y., Sze, K. H., Paine, M. J., Wolf, C. R., and Roberts, G. C. (1997) ^{1}H, ^{15}N and ^{13}C NMR resonance assignment, secondary structure and global fold of the FMN-binding domain of human cytochrome P450 reductase. *J. Biomol. NMR 10*, 63–75.
20. Garcin, E. D., Bruns, C. M., Lloyd, S. J., Hosfield, D. J., Tiso, M., Gachhui, R., Stuehr, D. J., Tainer, J. A., and Getzoff, E. D. (2004) Structural basis for isozyme-specific regulation of electron transfer in nitric-oxide synthase. *J. Biol. Chem. 279*, 37918–37927.
21. Kasim, M. (2002) Ph.D. Thesis, The Ohio State University, Columbus, OH.
22. Daff, S. N., Chapman, S. K., Turner, K. L., Holt, R. A., Govindaraj, S., Poulos, T. L., and Munro, A. W. (1997) Redox control of the catalytic cycle of flavocytochrome P-450 BM3. *Biochemistry 36*, 13816–13823.
23. Rock, D., and Jones, J. P. (2001) Inexpensive purification of P450 reductase and other proteins using 2′,5′-adenosine diphosphate agarose affinity columns. *Protein Expression Purif. 22*, 82–83.
24. Marohnic, C. C., Panda, S. P., Martasek, P., and Masters, B. S. (2006) Diminished FAD binding in the Y459H and V492E Antley-Bixler syndrome mutants of human cytochrome P450 reductase. *J. Biol. Chem. 281*, 35975–35982.
25. Clark, W. M. (1960) *Oxidation-reduction potentials of organic systems*, Williams & Wilkins, Baltimore.
26. Haines, D. C., Sevrioukova, I. F., and Peterson, J. A. (2000) The FMN-binding domain of cytochrome P450BM-3: Resolution, reconstitution, and flavin analogue substitution. *Biochemistry 39*, 9419–9429.
27. Dubourdieu, M., le Gall, J., and Favaudon, V. (1975) Physicochemical properties of flavodoxin from *Desulfovibrio vulgaris*. *Biochim. Biophys. Acta 376*, 519–532.
28. Chang, F. C., and Swenson, R. P. (1999) The midpoint potentials for the oxidized-semiquinone couple for Gly57 mutants of the *Clostridium beijerinckii* flavodoxin correlate with changes in the hydrogen-bonding interaction with the proton on N(5) of the reduced flavin mononucleotide cofactor as measured by NMR chemical shift temperature dependencies. *Biochemistry 38*, 7168–7176.
29. Mori, S., Abeygunawardana, C., Johnson, M. O., and van Zijl, P. C. (1995) Improved sensitivity of HSQC spectra of exchanging protons at short interscan delays using a new fast HSQC (FHSQC) detection scheme that avoids water saturation. *J. Magn. Reson., Ser. B 108*, 94–98.
30. Klein, M. L., and Fulco, A. J. (1993) Critical residues involved in FMN binding and catalytic activity in cytochrome P450BM-3. *J. Biol. Chem. 268*, 7553–7561.
31. Laskowski, R. A., MacArthur, M. W., Moss, D. S., and Thornton, J. M. (1993) PROCHECK: A program to check the stereochemical quality of protein structures. *J. Appl. Crystallogr. 26*, 283–291.
32. Vriend, G. (1990) WHAT IF: A molecular modeling and drug design program. *J. Mol. Graphics 8*, 52–56.
33. Nishimoto, K., Watanabe, Y., and Yagi, K. (1978) Hydrogen bonding of flavoprotein. I. Effect of hydrogen bonding on electronic spectra of flavoprotein. *Biochim. Biophys. Acta 526*, 34–41.
34. Sevrioukova, I., Truan, G., and Peterson, J. A. (1996) The flavoprotein domain of P450BM-3: Expression, purification, and properties of the flavin adenine dinucleotide- and flavin mononucleotide-binding subdomains. *Biochemistry 35*, 7528–7535.
35. Vervoort, J., Muller, F., Mayhew, S. G., van den Berg, W. A., Moonen, C. T., and Bacher, A. (1986) A comparative carbon-13, nitrogen-15, and phosphorus-31 nuclear magnetic resonance study on the flavodoxins from *Clostridium* MP, *Megasphaera elsdenii*, and *Azotobacter vinelandii*. *Biochemistry 25*, 6789–6799.
36. Witanowski, M., Stefaniak, L., and Webb, G. A. (1981) Nitrogen NMR spectroscopy. *Annu. Rep. NMR Spectrosc. 11B*, 1–493.
37. Moonen, C. T. W., Vervoort, J., and Muller, F. (1984) Reinvestigation of the structure of oxidized and reduced flavin: Carbon-13 and nitrogen-15 nuclear magnetic-resonance study. *Biochemistry 23*, 4859–4867.
38. Bradley, L. H., and Swenson, R. P. (2001) Role of hydrogen bonding interactions to N(3)H of the flavin mononucleotide cofactor in the modulation of the redox potentials of the *Clostridium beijerinckii* flavodoxin. *Biochemistry 40*, 8686–8695.
39. Cierpicki, T., and Otlewski, J. (2001) Amide proton temperature coefficients as hydrogen bond indicators in proteins. *J. Biomol. NMR 21*, 249–261.
40. Paine, M. J. I., Garner, A. P., Powell, D., Sibbald, J., Sales, M., Pratt, N., Smith, T., Tew, D. G., and Wolf, C. R. (2000) Cloning and characterization of a novel human dual flavin reductase. *J. Biol. Chem. 275*, 1471–1478.
41. Leclerc, D., Wilson, A., Dumas, R., Gafuik, C., Song, D., Watkins, D., Heng, H. H. Q., Rommens, J. M., Scherer, S. W., Rosenblatt, D. S., and Gravel, R. A. (1998) Cloning and mapping of a cDNA for methionine synthase reductase, a flavoprotein defective in patients with homocystinuria. *Proc. Natl. Acad. Sci. U.S.A. 95*, 3059–3064.
42. Sibille, N., Blackledge, M., Brutscher, B., Coves, J., and Bersch, B. (2005) Solution structure of the sulfite reductase flavodoxin-like domain from *Escherichia coli*. *Biochemistry 44*, 9086–9095.
43. Sharkey, C., Mayhew, S. G., Higgins, T. M., and Walsh, M. A. (1997) in *Flavins and Flavoproteins 1996* (Stevenson, K. J.,

Massey, V., and Williams, C. H., Jr., Eds.) pp 445−448, University of Calgary Press, Calgary, AB.

44. Romero, A., Caldeira, J., Legall, J., Moura, I., Moura, J. J., and Romao, M. J. (1996) Crystal structure of flavodoxin from *Desulfovibrio desulfuricans* ATCC 27774 in two oxidation states. *Eur. J. Biochem. 239*, 190–196.
45. Luschinsky, C. L., Dunham, W. R., Osborne, C., Pattriege, K. A., and Ludwig, M. L. (1991) in *Flavins and Flavoproteins 1990* (Curti, B., Ronchi, S., and Zanetti, G., Eds.) pp 409−413, W. de Gruyter, Berlin.
46. Kasim, M., and Swenson, R. P. (2000) Conformational energetics of a reverse turn in the *Clostridium beijerinckii* flavodoxin is directly coupled to the modulation of its oxidation-reduction potentials. *Biochemistry 39*, 15322–15332.
47. Draper, R. D., and Ingraham, L. L. (1968) A potentiometric study of the flavin semiquinone equilibrium. *Arch. Biochem. Biophys. 125*, 802–808.
48. Ishikita, H. (2008) Redox potential difference between *Desulfovibrio vulgaris* and *Clostridium beijerinckii* flavodoxins. *Biochemistry 47*, 4394–4402.
49. DeLano, W. L. (2002) *The PyMol Molecular Graphics System*, DeLano Scientific, San Carlos, CA.
50. Kurzban, G. P., and Strobel, H. W. (1986) Preparation and characterization of FAD-dependent NADPH-cytochrome P-450 reductase. *J. Biol. Chem. 261*, 7824–7830.

BI800954H